RSC Advances

ROYAL SOCIETY OF CHEMISTRY

www.rsc.org/advances

Curcumin loaded on pullulan acetate nanoparticles protects liver from the damages induced by DEN

Moorthy Ganeshkumar[a], Thangavel Ponrasu[a], Muthaiya Kannappan Subamekala[b], Murthy Janani[b] and Lonchin Suguna[a]

[a]Department of Biochemistry, CSIR-Central Leather Research Institute, Council of Scientific and Industrial Research, Adyar, Chennai-600020, India.

[b]Department of Biopharmaceutics, Anna University, Chennai, India.

Corresponding Author: Tel: (+) 91-44-24911386; Fax: (+) 91-44-24911589 slonchin@yahoo.co.uk, slonchin@hotmail.com (L.Suguna).

Abstract

In recent years, nanoparticles based drug delivery is being used to treat liver diseases. Even though curcumin is a potent antioxidant, reactive oxygen species (ROS) scavenger and anti-inflammatory agent, its use at clinical level is very limited due to its poor bioavailability rendered by its physiochemical property. In this study, biodegradable liver specific pullulan acetate nanoparticles (PA) loaded with curcumin were developed for the first time. These curcumin loaded PA nanoparticles were found to improve the encapsulation efficiency and stability of curcumin with sustained release, under physiological conditions. Thus, Curcumin loaded pullulan acetate nanoparticles (PAC) could solve the physicochemical defects of curcumin like solubility, pH stability, photo-stability, and be used as an effective hepato-protective agent against Diethyl nitrosamine (DEN) induced liver damages.

Key words: Pullulan acetate nanoparticles, curcumin, DEN, hepato-protective agent, zebrafish, antioxidant enzymes

1. Introduction

In liver, hepatocellular carcinoma is the most common cancer caused by hepatitis virus and other carcinogens. It has been estimated that 748,300 new cases and 695,900 deaths are reported every year due to hepatocellular carcinoma worldwide.[1] *N*-nitrosamines are a well-known group of carcinogens that can induce liver cirrhosis which leads to liver cancer. People who are exposed to unknown quantities of N-nitrosamines develop cancer as these are present in food, beverages, herbicides, pesticides and industrial pollution.[2] Metabolism of *N*-nitrosodiethylamine (DEN) in rats is similar to human and hence it is being used as a model carcinogen, to induce liver cancer. DEN produces many reactive metabolites that act together with DNA leading to the formation of DNA adducts, followed by mutations.[3] 8-hydroxyguanine is over expressed by the free radicals generated by DEN.[4] Excess amount of ROS accumulation causes damage to proteins, lipid, DNA, carbohydrates and membranes, resulting in oxidative stress and carcinogenesis.[5]

Chemoprevention is the best and perfect approach for the treatment of hepatic diseases. Curcumin, a natural polyphenolic compound, has been used as a drug for hepatocellular carcinoma in rat model [6,7] and hepato-protective agent against DEN.[8] However, pre-clinical to clinical applications for curcumin have not been developed successfully due to its poor bioavailability, low solubility, susceptibility for photolysis and pH dependent degradation. Targeted drug delivery systems based on nano formulations could provide permanent solutions for such problems.[9] Nano formulations developed by different methods[10,11] using natural, synthetic biocompatible polymers, like zein/quaternized chitosan,[12] PLGA,[13] biotin modified cholesteryl pullulan,[14] chitosan[15] and β-lactoglobulin[16] are being used to enhance the therapeutic efficacy of curcumin.

Pullulan is one such polysaccharide secreted by a fungus, *Aureobasidium pullulans*. It contains repeated malto-triose units, connected through α-1, 6 linkages. Due to its biocompatibility, it is recently being used for various biomedical applications including tissue engineering, targeted drug and gene delivery.[17] As pullulan is liver specific, it is exploited for targeting liver.[18-20] Pullulan shows a specific affinity for asialoglycoprotein receptors, which are greatly expressed on sinusoidal membranes of hepatocytes. Partial modification of pullulan by cholesterol produces amphiphilic properties which help in formation of self-assembled nanoparticles for delivering drugs to cells.[21, 22]

Pullulan acetate polymer could be used as a drug carrier, due to its non-toxic, non-immunogenic and biodegradable properties. It has high biocompatibility and solubility in a variety of organic solvents. Its good affinity towards the asialoglycoprotein receptor leads to receptor-mediated endocytosis that internalizes the pullulan to hepatocytes.[23, 24]

To improve the physicochemical properties of curcumin, curcumin loaded pullulan acetate nanoparticles have been synthesized for the first time. The nanoparticles thus prepared were characterized for particle size distribution, surface morphology and *in-vitro* drug release. Further, the hepato-protective efficacy of these nanoparticles against DEN induced liver damage was studied in rats.

2. Materials and methods

2.1. Material

Pullulan (MW = 200 kDa) was obtained as a gift sample from Hayashibara (Tokyo, Japan). Curcumin was purchased from Hi-media. Millipore milli Q water was used for all the experiments. All other chemicals and reagents were of analytical grade.

2.2. Methods

2.3. Synthesis of pullulan acetate

Pullulan acetate (PA) was produced by the method of Motozato.[25] Briefly; 2 g of pullulan was solubilized in 20 mL of formamide, and stirred strongly at 54ºC. To this solution, 6 mL of pyridine and 15 mL of acetic anhydride were added to change the degree of acetylation. The mixture was then stirred at 54°C for 48 h. A dark-brown precipitate thus obtained was purified by re-precipitation with 1000 mL of distilled water and 500 mL of methanol. The solid material was dried under vacuum for 24 h, and a white powder of pullulan acetate was obtained.

The degree of acetylation was found out by hydrolysis method.[26] In short, 0.5 g of the powder was accurately weighed and placed in a 250 mL Erlenmeyer Flask with stopper. To this 10 mL of reverse osmosis water, 25 mL of 0.1 N NaOH and a few drops of phenolphthalein were added. The mixture was stirred gently in a magnetic stirrer at room temperature for 2 h. Subsequently, the excess alkali was titrated with 0.1 N HCl until the pinkish red color of phenolphthalein disappeared. The same procedure was carried out for native starch. The DS was calculated using the following equation.

$$DS = (V_0 - V_1) \times N_{HCl} \times 162 \div (1000 \times m_M) - ((V_0 - V_1) \times N_{HCl} \times 42) \quad \text{.....(1)}$$

Where, V_0 is the titration volume of acid for the native starch (mL), V_1 is the titration volume of acid for the acetylated sample (mL), N_{HCl} is the normality of used HCl and m_M is the mass of the acetylated sample (g).

2.4. Formulation of curcumin loaded pullulan acetate nanoparticles (PAC)

The solvent diffusion method was used to prepare pullulan acetate nanoparticles.[22] In brief, 10, 20 and 30 mg of PA was mixed with 5 mg of curcumin and dissolved in 10 mL of acetone. This solution was then added drop wise to an aqueous solution containing various concentration of polyvinyl alcohol by means of a syringe under moderate stirring. Then the formulation was centrifuged at 4000 rpm for 10 minutes to remove free curcumin from nanoparticles loaded curcumin. Then, the free curcumin was dissolved in DMSO. Curcumin loading content was measured by UV-Visible spectroscopy method at 426 nm. The supernatant thus obtained was concentrated by centrifugation again at 13,000 rpm for 1 hour and the pellet was redispersed in water. Table s1 shows the optimization of PAC.

The percentage loading of curcumin in pullulan acetate nanoparticles was calculated using the following formula

$$\text{Loading efficiency} = \frac{\text{Amount of drug added during preparation} - \text{Amount of drug in the supernatant}}{\text{Amount of drug added during preparation}} \times 100$$

2.5. Characterization of pullulan acetate and curcumin loaded pullulan acetate nanoparticles

Fourier transform infrared (FTIR) spectra of pullulan, PA, and PAC were recorded using Perkin Elmer Fourier Transform Infrared Spectroscopy. The scan was performed in the range 4000-400 cm^{-1}. Surface morphology of PAC was carried out using Techni-20 Philips Transmission Electron Microscope operated at 80 kev. TEM samples were prepared by placing 2–3 drops of PAC solution on a copper grid and dried at room temperature after removing excess solution with filter paper. The particle size and distribution of drug-loaded PAC were elucidated by ZETASIZER (Malvern Instruments, Germany). The proton nuclear magnetic resonance (^{1}H NMR) spectra of PA and PAC were recorded on a Jeol spectrometer at 500MHz, using d-DMSO as a solvent.

2.6. Analysis of photo-physical properties

Encapsulation and binding efficiency of curcumin in PAC was further examined by spectroscopic analysis. We measured the absorbance and fluorescence spectra of curcumin

(dissolved in methanol) and PAC (in aqueous solution) at a concentration of 4 µg/mL. Curcumin was quantified spectrophotometrically at 426 nm and fluorescence emission spectra were recorded from 450 to 700 nm with an excitation wavelength of 420 nm.[27]

2.7. pH stability

To evaluate the pH stability of curcumin in curcumin loaded PA nanoparticles (PAC), the equal concentration of PAC (0.5 mL dispersed in aqueous solution) and 0.5 mL of free curcumin (dissolved in DMSO) were added to buffers with various pH (1.2, 4.5, 6.7, and 7.4). These solutions were incubated at 37°C for 6 h. Samples were removed periodically and the amount of pH stable free curcumin (curcumin without PA nanoparticles) and curcumin loaded in PA nanoparticles was analyzed spectrophotometrically at 426 nm.[28]

2.8. Photostability

To evaluate photo-stability, solutions of curcumin and PAC were kept in both ordinary and amber coloured bottles under normal light conditions. Sampling was done periodically and the amount of photostable curcumin in free curcumin and PAC was analyzed spectrophotometrically at 426 nm.

2.9. Solubility

To evaluate aqueous solubility of curcumin loaded in pullulan acetate nanoparticles against free curcumin, equivalent quantity of PAC and curcumin was dispersed in phosphate buffered saline (PBS, pH 7.4). Solubility of curcumin was compared visually and photographed.[27]

2.10. *In vitro* release

To find out *in vitro* release of curcumin from PAC, 2 mL of PAC was diluted in 10 mL of PBS (pH 7.4) and stirred in a magnetic stirrer at 37°C. At particular intervals, 0.5 mL of sample was taken and centrifuged at 4000 rpm for 10 minutes; the supernatant was poured into original solution. The pellet was redispersed in DMSO and the amount of curcumin released was determined spectrophotometrically at 426 nm. The experiment was performed in triplicate.

2.11. Hemolysis

Fresh blood was collected from healthy volunteers in sterile lithium heparin containers. RBCs were separated from whole blood by centrifugation at 1500 rpm for 10 minutes. The pellet containing RBCs was collected and diluted in PBS (pH 7.4) while the supernatant containing plasma and platelets was discarded. The RBCs were further washed three times with sterile PBS

solution. 1 mL of the RBCs pellet was re-suspended in 3 mL of PBS. Then 0.05 mL of diluted RBC suspension was added to 0.5 mL of PAC in PBS of different concentrations. After being slightly vortexed the suspension was stored at static condition for 4 h at 37°C. Then, the mixture was briefly vortexed again and centrifuged at 13,000 rpm for 10 minutes. The hemolysis was assessed by measuring absorbance of the supernatant at 575 nm. 0.05 mL of diluted RBC suspension was incubated with 0.5 mL of water and used as the positive control. The experiment was performed in triplicate. The percentage of hemolysis was calculated as follows.[29]

$$Hemolysis\ \% = 1/4 \frac{(sample\ absorbance - \ negative\ control)}{(positive - negative\ control)} \times 100$$

2.12. *In vivo* toxicity study of PAC in zebrafish embryo model

In vivo toxicity of PAC was assessed in zebrafish embryo model as mentioned in our previous report.[30] Briefly, fertilized eggs were collected from natural mating of adult zebrafish and embryos were gathered within 2 h of spawning. From the newly fertilized eggs approximately 2 h post fertilization (hpf), 10 healthy embryos were transferred to each well of a 24 well plate along with 1 mL of E3 medium. The embryos were exposed to different concentrations of curcumin and PAC, for 4 days. Tests were performed in duplicates. Embryos without treatment served as control. The dead embryos were removed immediately from the medium during the observation period and the remaining embryos were counted. At the end of the experiment, the larvae were transferred to a microscopic slide and then anesthetized with 0.016% tricaine. The preliminary morphological changes such as mortality rate, hatching rate, growth retardation and edema accumulation were monitored and photographed using an Olympus Stereo microscope.

2.13. *In vitro* antioxidant assay

In vitro antioxidant activity of the prepared PAC nanoparticles was determined using DPPH (2, 2'-Diphenyl-1-picrylhydrazyl). Various concentrations of PAC nanoparticles (2µg-10µg) were taken and 1 mL of DPPH (0.36 mM in ethanol) was added and kept in dark at room temperature for 20 minutes, then absorbance was measured at 517 nm. The values were expressed in µg equivalence of vitamin E, which served as the standard.[31]

2.14. Animals and grouping

Wistar albino rats weighing between 150-200 g, purchased from King Institute, Chennai, were used for the *in vivo* experiments. The rats were maintained in polypropylene cages under

controlled conditions of light/dark cycle (12:12 hrs), temperature at 29-31°C and fed with commercial rat feed and water *ad libitum*. All procedures were carried out according to the stipulations of the Institutional animal care and use committee (IACUC). A formal approval from the animal ethical committee has also been obtained.

Animals were divided into three groups each comprising of five rats. Group I animals served as the control. Groups II animals were administered with PAC orally, once a day for 4 consecutive days at a concentration of 20 mg/kg body weight. Group II and III animals were administered intraperitoneally with DEN at a concentration of 20 mg/kg body weight on 5th day.

After 48 h of DEN administration, all the animals were sacrificed and blood was collected. Liver tissue was also excised from the rats and washed completely with ice cold physiological saline to remove adhering blood and other tissues and stored at -20°C until used for the biochemical estimations.[32]

2.15. Lipid peroxidation assay

Liver tissue homogenate was taken to evaluate lipid peroxidation. The lipid peroxides (as malondialdehyde) were determined by thiobarbituric acid reaction.[33] and were expressed as nmoles of MDA/100 mg of wet liver tissue.

2.16. Assay for liver marker enzymes

Liver marker enzymes like aspartate transaminase (AST), alanine transaminase (ALT), alkaline phosphatase (ALP) and lactate dehydrogenase (LDH) were estimated in both serum and tissue homogenate to assess the liver function as reported earlier.[34-36]

2.17. Levels of antioxidants in liver tissue

Enzymatic and non-enzymatic antioxidants levels were determined in liver tissue homogenate. Enzymatic antioxidants like superoxide dismutase (SOD), catalase (CAT), glutathione peroxidase (GPx), glutathione-S-transferase (GST) and glutathione reductase (GR) were analyzed. Non-enzymatic antioxidants like reduced glutathione (GSH), vitamin E and vitamin C were also quantified as per standardized protocols in the literature.[37-43]

2.18. Statistics

Data were expressed as mean ± SD and the results were statistically evaluated using students paired t test and one-way ANOVA. All the statistical analyses were performed using graph pad prism (version 5.0; Graph Pad software Inc. San Diego CA, California, USA).

3. Results and discussion

3.1. Optimization and characterization of PAC

Pullulan, being a nonionic hydrophilic polymer, could be used as a carrier for many hydrophilic substances. But only a very small amount of hydrophobic compounds could be loaded due to its hydrophilic property. This problem could be overcome by making pullulan as pullulan acetate which is amphiphilic in nature, by acetylation process. PA can be self-assembled in to nanoparticles when exposed to non-solvent medium containing surfactants. The PA nanoparticles could be used as carriers for delivering drugs.[44-47]

The degree of acetylation was studied by hydrolysis method to confirm the formation of pullulan acetate from pullulan. The degree of substitution was found to be 4.96 and the % acetylation was found to be 57.62. These results confirm that our synthesis method is effective to form pullulan acetate. Percentage loading efficiency of curcumin in PA nanoparticle formulation is given in Table s2.

PAC formation was optimized by keeping the concentration of curcumin as constant but changing the concentration of PA and volume of aqueous phase with different strength of polyvinyl alcohol surfactants. Curcumin loading efficiency in PA nanoparticle was found to be in the range of 22.72 ± 1.02 to 85.87 ± 1.09 %. The formation of nanoparticles is possible within some moderate concentrations of PA as seen in Table s2. An increase in concentration of pullulan acetate in nanoparticle formulation leads to increased encapsulation efficiency of curcumin. Results of F6 and F7 in Table s1 showed little decrease in loading efficiency due to low concentration of the polyvinyl alcohol. As F5 found to have higher loading efficiency with 85.87 ± 1.09 %., further study was carried out using F5 formulation.

To confirm the presence of curcumin in pullulan acetate nanoparticles, FTIR analysis was carried out. Fig. s1a-c shows the FTIR spectra of pullulan, PA and PAC respectively. Pullulan consists of C-1, 4 and C-1, 6 glycosidic linkages and is a water-soluble, neutral, linear poly saccharide. In the present study, pullulan was modified by replacing the hydroxyl groups of the glucose unit with acetate groups to produce a hydrophobically modified pullulan, PA. The spectra demonstrated the introduction of acetate group, as indicated by C=O stretching at 1757cm^{-1}, CH_3 deformation at 1374cm^{-1}, and O–C=O bonds at 600cm^{-1}.[48]

Fig. s2 a-b shows ^{1}H NMR spectra of PA and PAC. Hydroxyl proton signals of PA at 4.5-5.6 ppm decreased when compared with that of pullulan, and methyl proton signals at 1.8-2.2 ppm, which are assigned to the acetyl groups, appeared in the ^{1}H NMR spectrum of PA. Some methine proton signals of pullulan shifted to lower magnetic field by acetylation. These results indicated that acetylation certainly occurred. No peaks of curcuminoids were observed in the spectra of PAC indicating the encapsulation of curcumin inside the nanoparticles was either in the form of molecular dispersion or amorphous. These results correlated with previously reported poly (butyl) cyanoacrylate nanoparticles loaded curcumin formulation.[49]

The surface morphology of the PAC formulation was measured using TEM (Fig. 1a). The nanoparticles in the formulation appeared almost spherical in shape as reported by Jung et al.[48] Particles size analysis of PAC is depicted in Fig.1b. Average particle size was in the range of 123.4 ± 2 nm. Measurement of the zeta potential values is the key indication for the stability of formulations. Results of zeta potential of PAC were in the range of -5.11 ± 1.0 which is shown in Fig. 1c. The lower value of zeta potential might be due to the non-ionic nature of pullulan.

To confirm the encapsulation as well as binding of curcumin in the hydrophobic core of PAC, the photo-physical property of curcumin is taken into consideration. Pure curcumin in methanolic solution illustrated a discrete high absorbance peak at around 425 nm. The absorbance peak of PAC was close to the absorbance peak of pure curcumin. This result confirmed the successful entrapment of curcumin within PA (Fig. 2a). Similarly, consistent to curcumin absorbance spectra, the fluorescence spectra also exhibited similar trends.

When the fluorescence spectra of curcumin (emission wavelength from 450 to 650 nm) with excitation wavelength 420 nm were observed, we found that pure curcumin in methanol solution illustrated a sharp fluorescence peak at 522 nm (Fig. 2b), but the fluorescence spectrum of PAC was shifted towards blue spectrum and showed a well-defined peak at 491 nm. This blue shift could be due to encapsulation of curcumin within hydrophobic domain of PA present in PAC.[50, 51] Similar results were observed in the formation of nano lipid carrier loaded drugs[52] and polymeric nanoparticle loaded curcumin.[53]

The solubility of PAC and curcumin was analyzed in PBS solution, pH 7.4. We found that PAC dispersed in aqueous solution gave a clear, well dispersed formulation with curcumin's natural color (Fig. 2c right inset), in contrast to native curcumin which was poorly soluble in

aqueous media as seen as microscopic undissolved flakes. (Fig. 2c left inset). Similar results were observed in glyceryl monooleate based nanoparticles loaded curcumin as reported by Mohanty & Sahoo.[27]

3.2. pH stability

One of the major challenges of drug delivery to cancerous tissue is its instability and biodegradation at physiological pH. 90% of curcumin was reported to get degraded in phosphate buffer at pH 7.4 within 30 mins.[51, 54] In an attempt to study the biodegradation and stability properties of curcumin, we incubated pure curcumin and PAC in PBS (pH 4.5 and 7.4), normal saline and E3 medium and estimated its concentration at different time intervals, spectrophotometrically.

Absorption spectra of PAC at various pH and time intervals were monitored for 24 h to know whether PA had any influence on the stability of curcumin and the results are shown in Fig 3. In the acidic pH of 4.5 (Fig. 3a), PAC was more stable than free curcumin. But at pH 7.4 (Fig. 3b), we observed only a minor change in the absorption maximum even after 8 h of incubation at 37°C. The results reflect the stability of PAC at physiological pH. However, from the degradation profile of pure curcumin we could observe that about 50% of degradation occurred within 2.5 h, which confirmed that pure curcumin underwent rapid degradation (only 22% of curcumin left intact after 24 h of incubation). Whereas, PAC was more stable under the same conditions i.e. 92% was found to be intact. PAC had more stability in saline (Fig. 3c), PBS and E3 medium (Fig. 3d) than curcumin. Thus, it is important to note that PA increased the stability of curcumin by encapsulation at various pHs so that PA could be used as a carrier for *in vivo* curcumin delivery.

3.3. Photostability

The photostability of PAC and curcumin is depicted in Fig. 3e. PAC was stable in both light and dark conditions, whereas pure curcumin was more stable only in dark. At the end of 6 h, there was no significant degradation of curcumin from PAC but pure curcumin showed 20% degradation when kept in light. The reduced rate of degradation of curcumin in PAC might be due to its presence inside the polymer matrix which provided protection from the damaging effect of light.

3.4. *In-vitro* drug release

The *in vitro* curcumin release behavior in PBS, (pH 7.4) was studied by dialysis method and shown in Fig. 3f. Curcumin was released from PAC in a biphasic pattern; a fast release rate in the first 1 h up to 39.36%, followed by a slow and uniform release. The initial burst of curcumin from nanoparticles suggested that some part of drug was adsorbed onto the surface of nanoparticles or loosely encapsulated in the hydrophilic domain of PA and the slow and uniform release could be caused by diffusion of the curcumin from PAC as observed by Ravi et al. for lopinavir loaded nanoparticles.[55] It was observed that curcumin showed sustained release (up to 80.95%) from PAC for 24 h.

Studying kinetics of encapsulated drug release from nanoparticles is important for biological activity. The drug release data were plotted in mathematical models according to the first order kinetic equation (r^2=0.794), Hixson and Crowell's equation (r^2=0.754), zero order equation (r^2=0.662), to study mass transport of drug that play a role in controlled drug release from nanoparticles. The kinetic studies of PAC showed that the release profile followed Korsmeyer-Peppas equation. The release of curcumin from PAC (F5) was by controlled diffusion mechanism which was further confirmed by the Korsmeyer-Peppas plots that showed fair linearity ($r^2 > 0.92$), with a slope value of 0.273, which was far less than 0.5.

3.5. Hemolysis

In vitro hemolysis of curcumin, PA and PAC was studied and the results are displayed in Fig. 4a, b. When the nanoparticles are injected into the blood stream for drug delivery or drug detoxification, detrimental interaction of these particles with blood constituents must be avoided. Nanoparticles used as carrier for drug delivery should be biocompatible with blood cell for *in vivo* application. Fig. 4a, b shows the hemolytic activities of PA nanoparticles (Fig. 4a), curcumin and PAC (Fig. 4b) dispersions at different concentrations.

The results showed that % hemolytic activity of PA nanoparticles increased with increase in concentration. At a concentration of 5.5 mg/mL, the hemolysis was below 5% indicating that any concentration below 5.5 mg/mL is suitable for parenteral application. Pure curcumin showed 4.139% hemolysis at 193.33 µg/mL; increasing the concentration above these limits lead to hemolysis more than 5%., whereas PAC demonstrated only 3.84% of hemolysis at 199.33 µg/mL concentration.

3.6. Zebrafish toxicity

Zebrafish is an ideal model to study vertebrate development, aquatic toxicology, human pathology and drug screening. Zebrafish embryos, possessing a high degree of homology to human genome, are good choice for all experiments for rapid high throughput and cost effective nanomaterials screening.[56] Zebrafish embryos are currently being used to screen the phenotypic and genotypic abnormalities when exposed to nanomaterials like metal oxide nanoparticles and gold nanoparticles.[30, 57] So we have used the embryo model to screen the toxic effect of different concentrations of PAC.

Generally, growth, total length, body shape, heart, pericardial sac, facial edema, pigmentation, tail shape, tail length and presence of swim bladder are considered as the key markers to evaluate the toxicity during zebrafish development. In addition, hatching rate, survival rate and mortality are crucial to detect the toxicity of the prepared nanoparticles. [56]

Pure curcumin at a concentration of 15 µg showed no morphological changes like total length, body shape, heart, pericardial sac, facial edema, pigmentation, tail shape, tail length and hatching rate. However, a decrease in survival rate (17%) was observed at this concentration. Even though there were no changes observed in morphology and hatching rate, a slight decrease in the survival rate (14%) was only observed in PAC treated embryos at a concentration of 56.85 µg because of the sustained and controlled release of curcumin from PAC [(as seen in Fig. 5a, b (hatching rate), Fig. 5c, d (percentage survival rate) and Fig. 6a, b (morphological analysis)]. Hence, PAC can be used as a potential candidate for the sustained curcumin delivery for various biomedical applications.

3.7. DPPH assay

The free radical scavenging ability of the free curcumin and PAC was determined in both DMSO and PBS, pH 7.4 (Fig. 7a). Results are expressed in vitamin E equivalence. PAC in PBS showed high antioxidant potential when compared to free curcumin in PBS (more than 90%). This confirmed that the encapsulation of the curcumin molecule in to PAC did not affect the antioxidant property of curcumin. This is due to the improved solubility of hydrophobic curcumin in PA nanoparticles by exposing larger surface area to aqueous medium.[58]

3.7.1. Lipid peroxidation assay

Reactive oxygen species (ROS) and free radicals cause membrane damage and lead to excessive formation of malondialdehyde (MDA) in tissues. To assess the lipid peroxidation, MDA level

was estimated in experimental animals and showed in Fig. 7b. PAC treatment showed 38% ($p < 0.001$) of decreased lipid peroxidation when compared to DEN induced untreated animals confirming the antioxidant nature of curcumin. This is probably due to the presence of active chemical groups like hydroxyl, methoxy and 1, 3 di ketone conjugated diene in curcumin molecule.[59] Ghosh et al. reported that PLGA- nanocurcumin prevented ROS production and thus reduction in lipid peroxidation.[8]

3.8. Assay for liver marker enzymes

Liver damage affects the normal liver metabolism leading to elevated levels of intracellular liver enzymes such as AST, ALT, ALP and LDH. These are the key enzymes to diagnose normal liver function. Increased levels of these enzymes in both serum and liver tissues represent the extent of hepatocellular damage. Liver marker enzymes were quantified in both serum and liver for all the experimental groups. Fig. 7c shows the levels of these enzymes present in serum.

PAC treatment significantly ($p < 0.05$) reduced the levels of AST (39%), ALT (18%), LDH (41%) and ALP (5%) in serum. The levels of these enzymes in liver tissue homogenate were estimated and expressed in Fig. 7d. Significant reduction in AST (23%), ALP (26%), LDH (34%) and ALT (9%) was observed in liver tissue.

Liver injury alters the membrane permeability and transport function of the liver leading to excessive leakage of these enzymes.[60] Elevated levels of AST and ALT in the serum indicated cell damage in DEN induced animal. Treatment with PAC significantly decreased the AST and ALT levels in serum. This is probably due to the protective nature of PAC by preserving the structural integrity of hepatocellular membrane against DEN. Tetrahydrocurcumin treatment also showed similar results as reported by Pari et al.[61]

Increased level of ALP, also known as cholestatic liver enzyme, might be due to a condition called chloestasis caused by DEN. Increased biliary pressure lead to the elevation of ALP in serum, which affected the function of hepatic cells.[62] PAC treatment reduced the ALP in serum due to an early improvement in secretory mechanism of hepatic cells. Increase in LDH activity indicated the significant cellular damage.[63] A notable reduction in LDH activity observed in PAC treated rats confirmed its protective nature against excessive cellular damage.[64]

3.9. Levels of antioxidants in liver tissue

Antioxidants are the first line defense mechanism against oxidative damage. Fig. 8a shows the levels of enzymatic antioxidants present in liver tissue for all the experimental animals. Increased levels of enzymatic antioxidants like SOD (29%), CAT (41%), GST (26%) and GPx (35%) were observed in PAC treated groups than the untreated group. Similar trend was observed for the non-enzymatic antioxidants like GSH (21%), Vit-E (7%) and Vit-C (10%).

SOD catalyses the dismutation of superoxide radicals and plays a primary role in defense mechanism. Decreased activity of SOD may result in a number of harmful effects in cells due to the accumulation of superoxide anion. Inactivation of hydrogen peroxide or glycation of the enzyme causes decreased SOD activity.[65] Administration of PAC increased the activities of SOD in DEN induced rats.

CAT, a heme protein, catalyses hydrogen peroxides and protects the healthy tissues from hydroxyl radical attack. Decreased activity of catalase leads to accumulation of hydrogen peroxides in tissues. PAC increased the catalase activity and reduced the cell damage in treated animals. Glutathione-S-transferase is a group of multifunctional proteins that play a central role in detoxification of electrophilic chemicals and help the hepatic cells to remove potentially harmful hydrophobic compounds from blood. Results showed a significant increase in GST level in PAC treatment when compared to DEN treated rats.

GPx plays an important role by scavenging peroxyl radicals and maintaining the functional integration of cell membranes. The activity of GPx was significantly raised in PAC treated rats. This is due to the induction GPx by PAC to encounter the harmful effect of DEN. Nrf2 is considered as a redox-sensitive transcription factor. Curcumin is involved in the induction of Nrf2 thereby protecting the cells from oxidative damage indirectly. This is probably due to the presence of keto-enol functional moieties in the aromatic system of the curcumin molecule. Curcumin also up-regulates the genes to promote the antioxidant response elements including SOD, CAT, GST, GPx and GR.[66]

Non-enzymatic antioxidants such as reduced glutathione, vitamin C and vitamin E have an important role to play in protecting the cells from oxidative damage. Fig. 8b shows the levels of non- enzymatic antioxidants present in liver tissue for all the experimental animals. Glutathione, a cysteine-containing molecule, synthesized in cells acts as an effective antioxidant to maintain the cellular antioxidant capacity due to the presence of thiol group in its cysteine

moiety.[67] GSH plays an essential role in detoxification of foreign compounds like DEN. GSH donates the thiol group to electrophilic site and neutralizes the free radical.[8]

Vitamin E, the most important antioxidant present in animal cells, protects the cells against carcinogenesis and tumor growth.[68] Vitamin E level was drastically decreased in untreated group. This is due to the excessive utilization of this molecule to quench the free radicals formed enormously due to DEN treatment. However, near normal level of vitamin E was found in PAC treated animals due to the scavenging activity of curcumin and thus maintaining the normal level of vitamin E in rats.

Vitamin C protects the cell membranes and lipoprotein particles from oxidative damage by regenerating the antioxidant in form of vitamin E.[69] Hence, vitamin C and vitamin E synergistically act as barrier for a variety of reactive oxygen species (ROS). In PAC treated rats, vitamin C was found to be in near normal level. This is due to the regeneration of ascorbic acid in PAC treated group and the potent antioxidant activity of PAC. Free radical scavenging ability of curcumin was well documented for a variety of ROS and free radicals. This is because of the presence of phenolic β-diketone and methoxy functional groups in curcumin moiety. Curcumin protects the liver from fibrogenesis and oxidative damage by suppressing inflammation and increasing the xenobiotic detoxifying enzymes significantly.[70, 71]

DEN induced hepatocellular toxicity was also assessed histologically for all the groups by staining the liver tissues with Hematoxylin-Eosin (H&E) and examined under light microscope. Control group without any treatment (Fig. 8c, d) showed normal liver cell architecture with uniform nuclei, hepatic and portal veins. DEN treated tissues (Fig. 8e, f) showed cells without cytoplasm with abnormal nuclei and complete loss of architecture. Excess nodular formation, enlarged hepatic veins with cluster of tumor thrombi within the hepatic and portal veins were also observed. DEN + PAC treated liver tissues (Fig. 8g, h) showed uniform size of nuclei, less number of nodules and normal structure of hepatic veins. PAC treatment improved the architecture of hepatocytes as normal cells.

Curcumin is also involved in the inhibition of hepatic stellate cells activation and increase the mitochondrial function to protect the liver.[72] Encapsulation of curcumin into nano formulation increases the efficacy and solubility and reduces the dose requirement for protective effect.[60]

The main aim of this investigation was to improve the physicochemical property of curcumin for its use in various biomedical applications. In this study, we have focused mainly on improving the solubility of curcumin. Hence, we compared only native curcumin (solution) with curcumin loaded pullulan acetate nanoparticles, not with PA nanoparticles. Tang et al. (2010) have reported in an *in vivo* study that pullulan acetate nanoparticles (PANs) were stable, safe, nontoxic and potential carriers to improve the bioavailability of the loaded drug. Therefore, we did not compare the results with empty nanoparticles.[73] Overall, these results strongly substantiate that PAC is more potent to reduce the toxic effects of DEN than free curcumin.

4. Conclusion

Liver specific pullulan acetate nanoparticles loaded curcumin (PAC) were synthesized for the first time. The loading efficiency was found to be 85.87 ± 1.09 %. The average particles size of PAC was in the range of 123.4 ± 2 nm. PAC thus prepared showed bi-phasic and diffusion controlled curcumin release. PAC improved physiochemical property and stability of curcumin under physiological conditions. PAC showed good hemocompatability in *in vitro* and biocompatibility in zebrafish embryos. DEN administration increased the mitochondrial ROS with substantial reduction of enzymatic and non-enzymatic antioxidants in hepatic tissue and induced hepatocarcinoma in rat. PAC significantly reduced the liver marker enzyme levels in both serum and liver tissue. Non-enzymatic antioxidants levels were also increased considerably. These results were well supported by the histopathological evaluations. Based on the results obtained, PAC could be used as a therapeutic agent for hepatic diseases in the near future.

Acknowledgement

M. Ganeshkumar and T. Ponrasu would like to acknowledge the Council of Scientific and Industrial Research (CSIR), New Delhi, for granting Senior Research Fellowship and financial support. Pullulan received as gift sample from Hayashibara (Tokyo, Japan) is gratefully acknowledged by all the authors. The authors thank Dr. M.D. Naresh (Biophysics Lab in CLRI) for help in the microscopic technique. The authors thank Central Instrumentation Lab, Tamilnadu Veterinary and Animal Science University for help in the TEM analysis.

References

1 A. Jemal, F. Bray, M. M. Center, J. Ferlay, E. Ward, D. Forman. *CA Cancer J Clin*., 2011, **61,** 69-90.

2 Colin Crews. *Quality Assurance and Safety of Crops & Foods*., 2010, **2,** 2–12.

3 M. C. Dyroff, F.C.Richardson, J. A. Popp. *Carcinogenesis.,* 1986, **7,** 241– 246.

4 D. Nakae, Y. Kobayashi, H. Akai, N. Andoh, H. Satoh, K. Ohashi, M. Tsutsumi, Y. Konishi.. *Cancer Res*., 1997, **57,** 1281–1287.

5 R.T. Dean, S. Fu, R. Stocker, M. J. Davies. *Biochem J.*, 1997, **324,** 1–18.

6 Khemraj Bairwa, Jagdeep Grover, Mihir Kania and Sanjay M. Jachak . *RSC Adv*., 2014, **4,** 13946-13978.

7 Altaf S. Darvesh, Bharat B. Aggarwal, and Anupam Bishayee. *Curr Pharm Biotechnol.,* 2012, 13, 218-228.

8 D. Ghosh, S. T. Choudhury, S. Ghosh, A. K. Mandal, S. Sarkar, A. Ghosh, K. D. Saha, N. Das. *Chem Biol Interact*., 2012, **195,** 206-214.

9 L. Giannitrapani, M. Soresi, M. L. Bondì, G. Montalto, M. Cervello. *World J Gastroenterol*., 2014, **20,** 7242-7251.

10 O. Naksuriya, S. Okonogi, R. M. Schiffelers, W. E. Hennink. *Biomaterials*., 2014, **35,** 3365-3383.

11 W. H Lee, C.Y Loo, P. M. Young, D. Traini, R. S. Mason, R. Rohanizadeh. *Expert Opin Drug Deliv*., 2014, **11,** 1183-1201.

12 Hongshan Liang, Bin Zhou, Lei He, Yaping An, Liufeng Lin, Yan Li, Shilin Liu, Yijie Chen and Bin Li. *RSC Adv.,* 2015, **5,** 13891-13900.

13 M. Sampath, R. Lakra, P. Korrapati, B. Sengottuvelan. *Colloids Surf B Biointerfaces*., 2014, **117,** 128-134.

14 W. Yang, M. Wang, L. Ma, H. Li, L. Huang. *Carbohydr Polym*., 2014, **99,** 720-727.

15 L. H. Chuah, C. J. Roberts, N. Billa, S. Abdullah, R. Rosli. *Colloids Surf B Biointerfaces*., 2014, **116,** 228-236.

16 N. P. Aditya, H. Yang, S. Kim, S. Ko. *Colloids Surf B Biointerfaces*., 2015, **127,** 114-121.

17 R. S. Singh, N. Kaur, J.F. Kennedy. Carbohydr *Polym*., 2015**, 123,** 190-207.

18 M. Ganeshkumar, T. Ponrasu, M. D. Raja, M. K. Subamekala, L. Suguna. *Spectrochim acta A: Mole biomol spectrosc,* 2014, **130,** 64 –71.

19 J. H. Kang, Y. Tachibana, W. Kamata, A. Mahara, M. Harada-Shiba, T.Yamaoka. *Bioorg Med Chem.,* 2010, **18,** 3946-3950.

20 Huanan Li, Yong Sun, Jie Liang, Yujiang Fan and Xingdong Zhang *J. Mater. Chem. B.,* 2015, Advance Article DOI: 10.1039/C5TB01210D

21 S. J. Lee, G. Y. Hong, Y. I. Jeong, M. S. Kang, J. S. Oh, C. E. Song, H. C. Lee. *Int J Pharm.,* 2012, **433,** 121-128.

22 H.Z. Zhang, F.P. Gao, L.R. Liu, X.M. Li, Z.M. Zhou, X.D. Yang, Q.Q. Zhang. *Colloids Surf B Biointerfaces.,* 2009, **71,** 19-26.

23 Y. Kaneo, T.Tanaka, T.Nakano, Y.Yamaguchi. *J Control Release*., 2001, **70,** 365-373.

24 K. Xi, Y. Tabata, K. Uno, M. Yoshimoto, T. Kishida, Y. Sokawa, Y. Ikada. *Pharm Res*., 1996, **13,** 1846-1850.

25 Y. Motozato, H. Ihara, T. Tomoda, and C. Hirayama, *J Chromatogr.,* 1986, **355,** 434-437.

26 Henky Muljana, Francesco Picchioni, Hero J. Heeres, Leon P. B. M. Janssen. *Carbohydr. Polym.,* 2010, **82,** 653–662.

27 C. Mohanty, S. K. Sahoo. *Biomaterials*., 2010, **31,** 6597-6611.

28 Ashok Patel, Yingchun Hu, Jyoti Kumar Tiwari and Krassimir P.Velikov. *Soft Matter.*, 2010, **6,** 6192–6199.

29 Xiangsheng Liu, Qiao Jin, Ying Ji and Jian Ji. *J. Mater. Chem.,* 2012, **22,** 1916-1927.

30 M. Ganeshkumar, M. Sathishkumar, T. Ponrasu, M. G. Dinesh, L. Suguna. *Colloids Surf B Biointerfaces*., 2013, **106,** 208– 216.

31 R. E. Charles, T. Ponrasu, R. Sivakumar, S. Divakar. *Biotechnol Appl Biochem*., 2009, **52,** 177-84.

32 E. O. Farombi, S. Shrotriya, H. K. Na, S. H. Kim, Y. Surh. J. *Food Chem Toxicol*., 2008, **46,** 1279-87.

33 M. A. Santos, M. Pacheco, I. Ahmad. *Chemosphere*., 2006, **63,** 794-801.

34 J. King. In: King J (Ed) *Practical clinical enzymology*., D Van Nostrand Company Ltd, London, 1965, 83–93.

35 J. King. In: King J (Ed) *Practical clinical enzymology*., D Van Nostrand Company Ltd, London, 1965, 121–138.

36 S. B. Rosalki, D. Rau. *Clin Chim Acta*., 1972, **39,** 41–47.

37 S. Marklund, G. Marklund. *Eur J Biochem*., 1974, **47,** 469–474.

38 A.K.Sinha. Colorimetric assay of catalase. *Anal Biochem*., 1972, **47,** 389–394.

39 J. T. Rotruck, A. L. Pope, H. E. Ganther, A. B. Swanson, D. G. Hafeman, W. G. Hoekstra. *Science*., 1973, **179,** 588–590.

40 M.S. Moron, J.W. Depierre, B. Mannervik. *Biochim Biophys Acta*., 1979, **582,** 67–78.

41 H. D Horn, F. H. Burn. In: Bergmeyer HV (ed) *Methods in enzymology*., Academic Press, New York, 1978, 877.

42 I. D. Desai. *Methods Enzymol.,* 1984, **105,** 138–147.

43 S.T. Omaye, J. D. Turnbull, H. E Sauberlich. *Methods Enzymol*., 1979, **62,** 3–11.

44 H. Z. Zhang, X. M. Li, F. P. Gao, L. R. Liu, Z. M. Zhou, Q. Q. Zhang. *Drug Deliv*., 2010, **17,** 48-57.

45 H. B. Tang, L. Li, H. Chen, Z. M. Zhou, H. L. Chen, X. M. Li, L. R. Liu, Y. S. Wang, Q. Q. Zhang. *Drug Deliv*., 2010, **17,** 552-558.

46 H. Z. Zhang, F. P. Gao, L. R. Liu, X. M. Li, Z. M. Zhou, X. D. Yang, Q. Q. Zhang. *Colloids Surf B Biointerfaces*., 2009, **71,** 19-26.

47 Franco Alhaique, Pietro Matricardi, Chiara Di Meo, Tommasina Coviello, Elita Montanari. *J Drug Deliv Sci Tec.,* 2015, 1-10. 10.1016/j.jddst.2015.06.005.

48 S.W.Jung, Y. I. Jeong, S. H. Kim. *Int. J. Pharm*., 2003, **254,** 109 – 121.

49 R. Mulik, K. Mahadik, A. Paradkar. *Eur J Pharm Sci*., 2009, **37,** 395-404.

50 S. Manju, K. Sreenivasan. *J Colloid Interface Sci*., 2011, **359,** 318-325.

51 Y. J. Wang, M. H. Pan, A. L. Cheng, L. I. Lin, Y. S. Ho, C. Y. Hsieh. *J Pharm Biomed Anal*., 1997, **15,** 1867-1876.

52 F. Meng, S. Asghar, S. Gao, Z. Su, J. Song, M. Huo, W. Meng, Q. Ping, Y. Xiao. *Colloids Surf B Biointerfaces*., 2015, **134,** 88-97.

53 C. Banerjee, S. Maiti, M. Mustafi, J. Kuchlyan, D. Banik, N. Kundu, D. Dhara, N. Sarkar. *Langmuir*., 2014, **30,** 10834-10844.

54 Z. Ma, A. Haddadi, O. Molavi, A. Lavasanifar, R. Lai, J. Samuel. *J Biomed Mater Res A*., 2008, **86,** 300-310.

55 P. R. Ravi, R. Vats, J. Balija, S. P. Adapa, N. Aditya. *Carbohydr Polym*., 2014, **110,** 320–328.

56 S. M. Bugel, R. L. Tanguay, A. Planchart. *Curr Environ Health Rep*., 2014, **1,** 341-352.

57 L. C. Wehmas, C. Anders, J. Chess, A. Punnoose, C. B. Pereira, J. A. Greenwood, R. L. Tanguay. *Toxicol Rep*., 2015, **2,** 702-715.

58 S. Bisht, G. Feldmann, S. Soni, R. Ravi, C. Karikar, A. Maitra. *Journal of Nanobiotechnology .,* 2007, 5:3

59 J. Trujillo, Y. Chirinio, E. Molina-Jijón, C. Andérica-Romero, E. Tapia, J. Pedraza-Chaverrí,. *Redox Biol.,* 2013, **1,** 448–456.

60 G. Shatadal, B. Sudip, R. Kahkashan, C. S. Parames. *Toxicol Rep.,* 2015, **2,** 365–376.

61 L. Pari, P. Murugan. *Pharmacol Res*., 2004, **49,** 481-486.

62 P. Muriel, T. Garciapina, V. Perez-Alvarez, M. Mourelle. *J Appl Toxicol.,* 1992, **12,** 439-442.

63 G. Konjevic , V. Jurisic , B. Jakovljevic , I. Spuzic . *Glas Srp Akad Nauka Med.,* 2002, **47,** 137-147.

64 S. K. Hassan, A. M. Mousa, M. G. Eshak, A. E. H. H. Farrag, A. E. F. M. Badawi. *Int J Pharm PharmSci*., 2014, **6,** 54-62.

65 S. Das, S. Vasisht, R. Snehlata, N. Das, L. M. Srivastava. *CurrSci.*, 2000, **78,** 486-487.

66 W. R García-Niño, J. Pedraza-Chaverrí. *Food Chem Toxicol*., 2014, **69,** 182-201.

67 C. Gupta, A. Vikram, D.N. Tripathi, P. Ramarao, G.B. Jena. *Phytother. Res.,* 2010, **24,** 119–128

68 S. Das. *Acta Oncol*., 1994, **33,** 615-619.

69 G. R. Buettner. *Arch. Biochem. Biophys*., 1993, **300,** 535-543.

70 N. Mathuria, R. Verma. *Acta Pol. Pharm*., 2007, **63,** 413–416.

71 H. Farghaly, M. Hussein. *J. Basic Appl. Sci*., 2010, **4,** 4266–4274.

72 S. Priya, P. Sudhakaran. *Indian J. Biochem. Biophys*., 2008, **45,** 317–325.

73 H. B. Tang, L. Li, H. Chen, Z. M. Zhou, H. L. Chen, X. M. Li, L. R. Liu, Y. S. Wang, Q. Q. Zhang. *Drug Deliv.* 2010, **17,** 552-558.

Figure captions

Figure 1. (a). TEM analysis of PAC (b) Particle size analysis of PAC (c) Zeta potential of PAC

Figure 2. (a) UV/Visible absorbance spectra of PAC and curcumin. (b). Fluorescence emission spectra of PAC and Curcumin (c). Solubility of PAC and curcumin in PBS, pH 7.4

Figure 3. *In vitro* stability of PAC and curcumin in (a) pH 4.5 (b) pH 7.4 (c) saline (d) E3 medium (e) photostability of PAC and curcumin (f) *In vitro* drug release from PAC.

Figure 4. (a). *In vitro* hemolysis of PA (b). Curcumin and PAC. Values are expressed as mean ± SD (n=3) and the level of significance is denoted as *p < 0.05, compared with positive control (water).

Figure 5. Percentage hatching rate of PAC and curcumin (a, b). Percentage survival rate of PAC and curcumin (c, d).

Figure 6. Morphological analysis of curcumin (a) and PAC treated zebrafish embryos (b).

Figure 7. (a) *In vitro* DPPH scavenging ability of curcumin and PAC in DMSO and PBS at pH 7.4. (b) Level of lipid peroxides measured as MDA in both DEN and DEN + PAC treated liver. The results are expressed as mean ± SD (n=3) and the level of significance is denoted as ***p < 0.001, compared with corresponding control. (c) Activities of marker enzymes like AST, ALT, ALP and LDH in serum. (d) Activities of marker enzymes in liver. Values are expressed as mean ± SD (n=3) and the level of significance is denoted as *p < 0.05, compared with corresponding control.

Figure 8. (a) Levels of enzymatic antioxidants in liver tissue of control and experimental rats. Activity units for SOD: superoxide dismutase in units/mg protein; CAT: catalase in µmol of H_2O_2 consumed/min/mg protein, GST: µmol of CDNB conjugated/min/mg protein and GPx: µmol of GSH oxidized/min/mg protein respectively. (b) Levels of non-enzymatic antioxidants in liver tissue. Activities are expressed as mg/100 mg tissue. Values are expressed as mean ± SD (n=3) and the level of significance is denoted as **p < 0.01; *p < 0.05, compared with corresponding control. Histopathological examination of DEN induced, DEN + PAC treated and normal liver tissue (Stained with Hematoxylin-Eosin (H&E); magnification 20 x; scale bar 50 µm). Control group (c, d) showing normal liver cell architecture with uniform nuclei, hepatic and portal veins. The liver of DEN induced group (e, f) showing complete loss of architecture, cells without cytoplasm with abnormal nuclei. Also, we observed significant nodular formation,

enlarged hepatic veins with cluster of tumor thrombi within the hepatic and portal veins. Liver of PAC treated rats (g, h) showing uniform size of nuclei, less number of nodules and normal structure of hepatic veins. Hepatocytes were in cytologically similar architecture as normal liver cells.

Figure 1

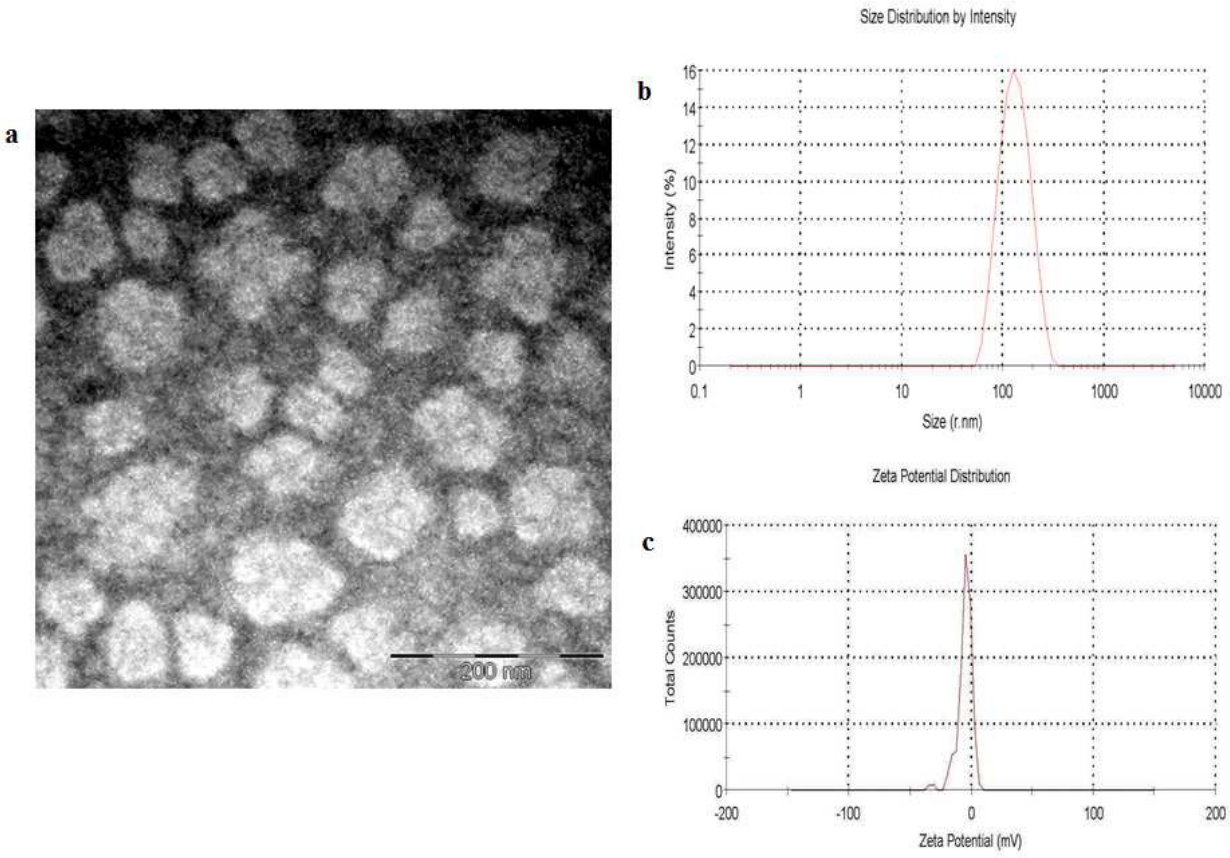

Figure 2

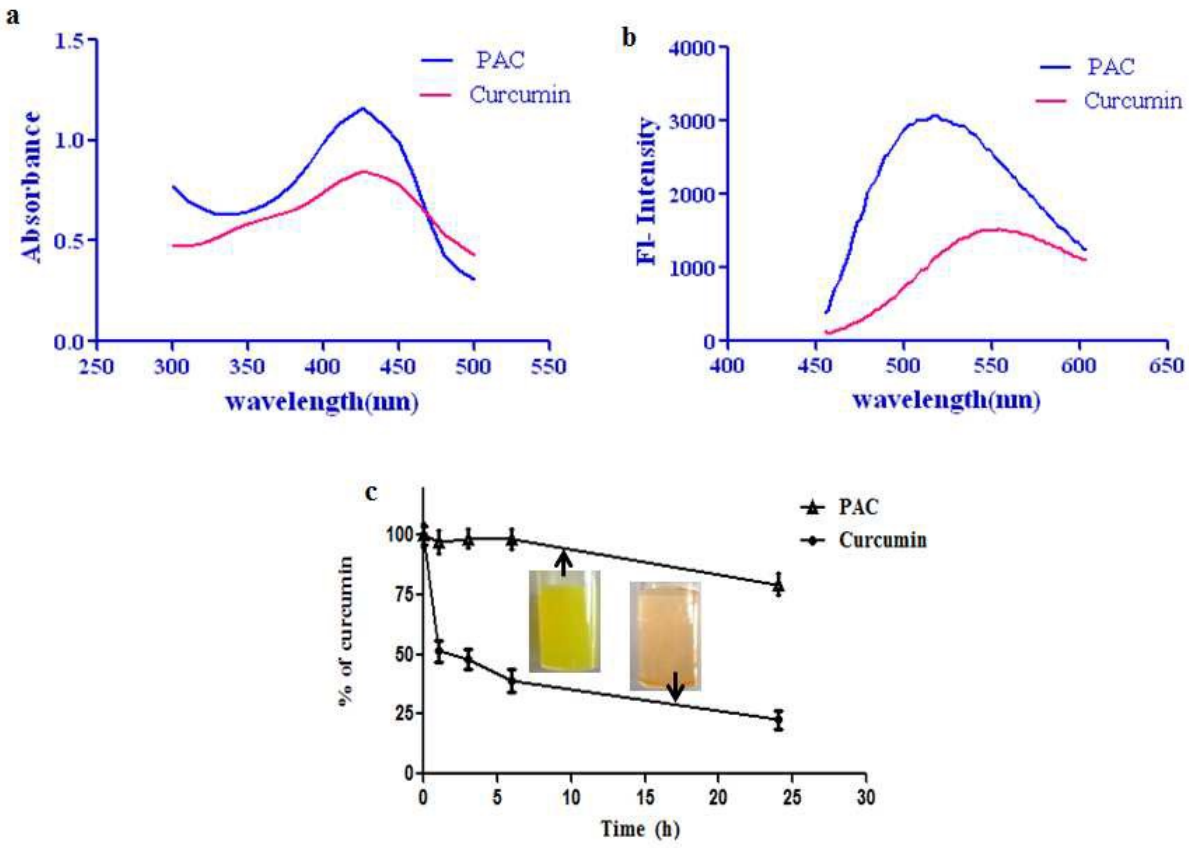

Figure 3

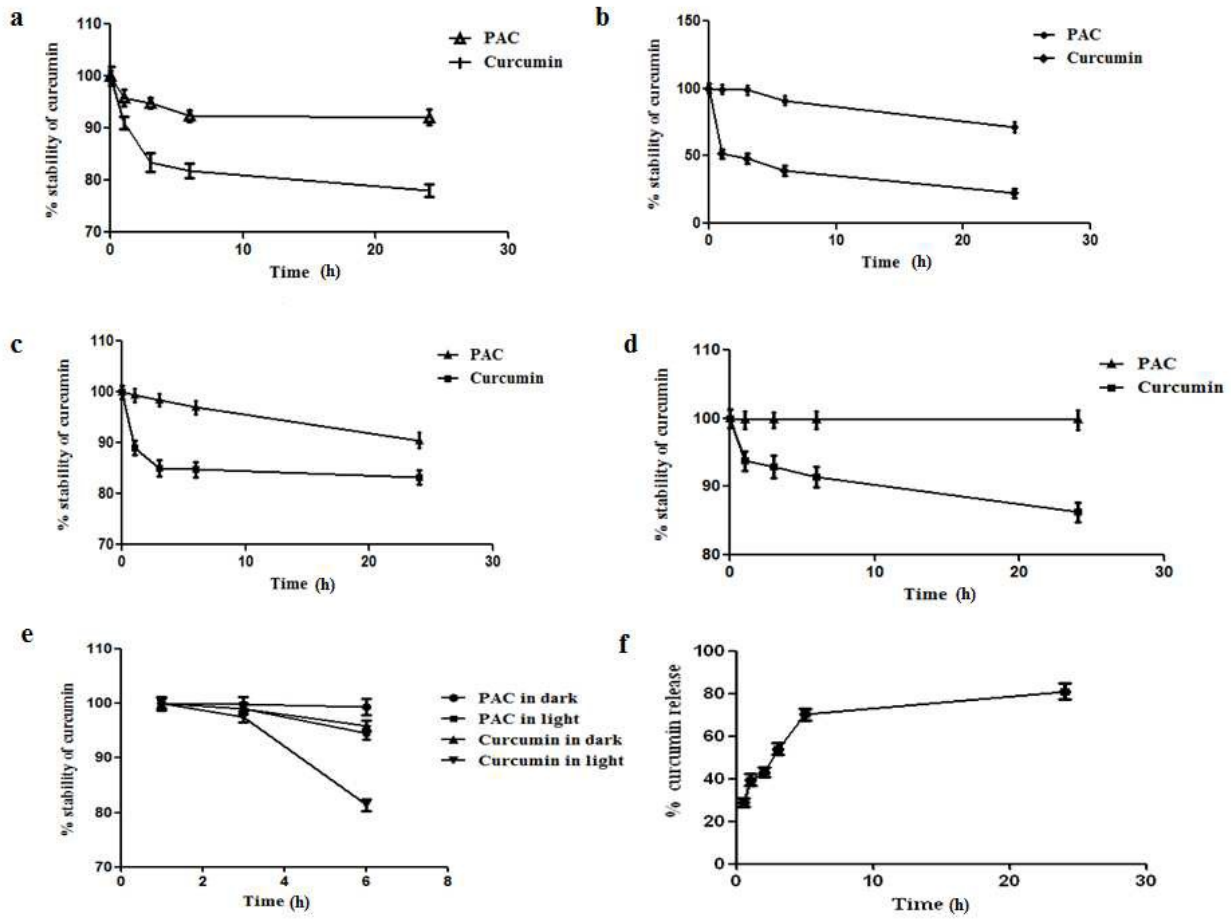

Figure 4

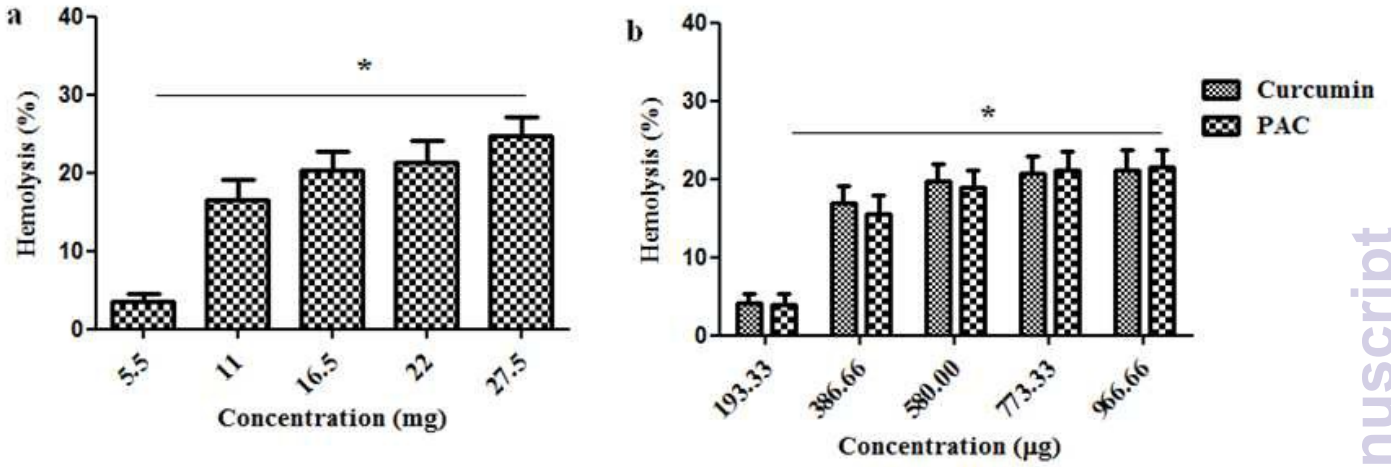

Figure 5

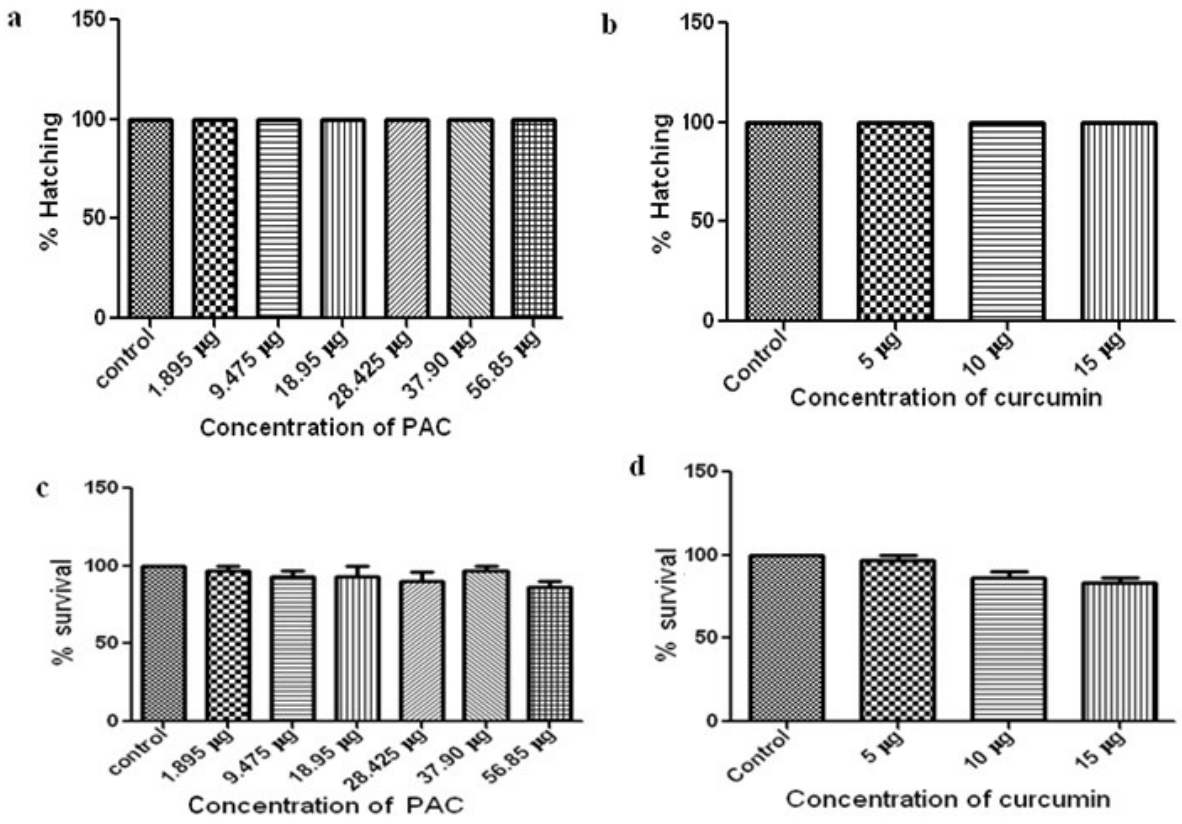

Figure 6

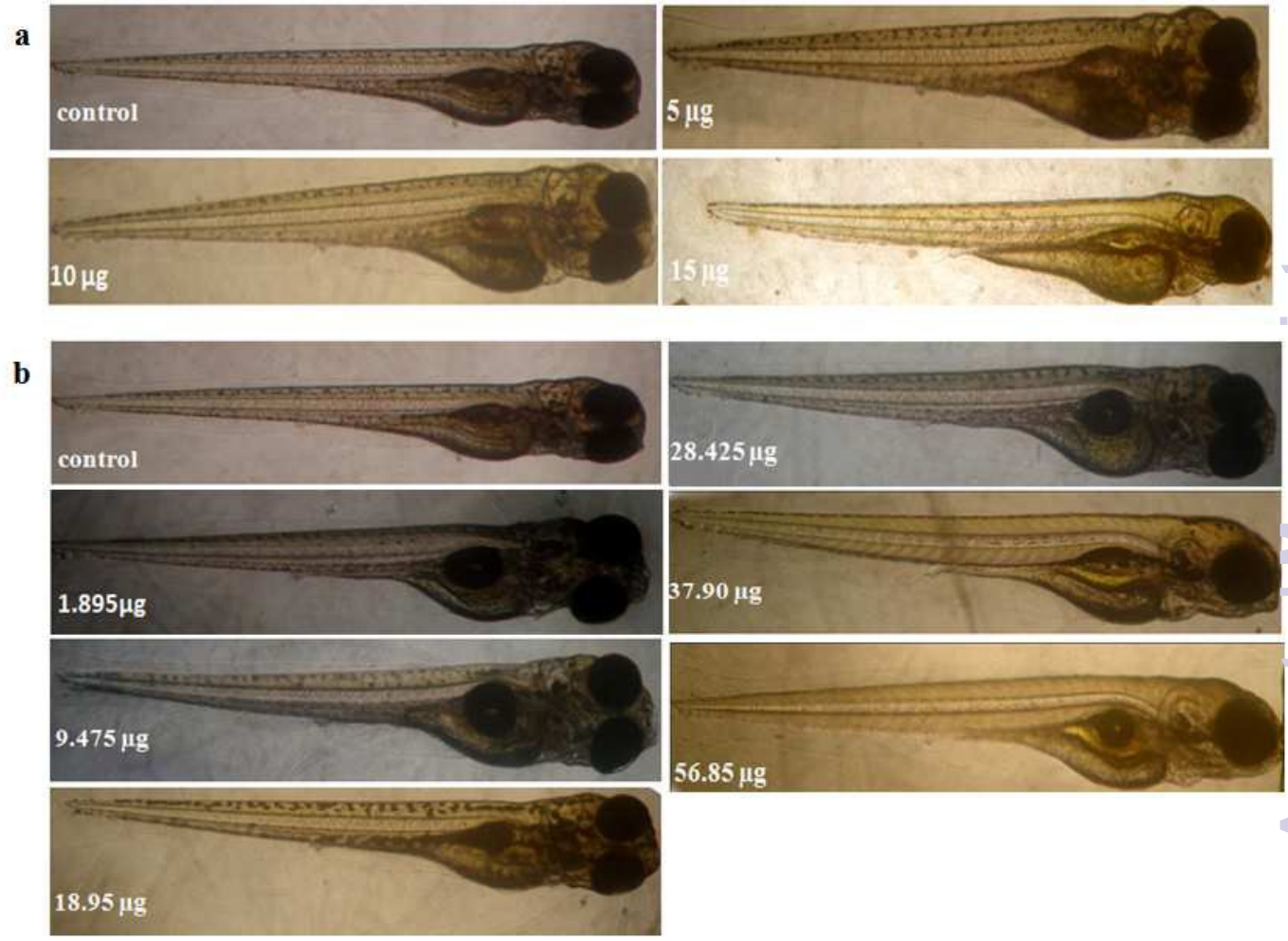

Figure 7

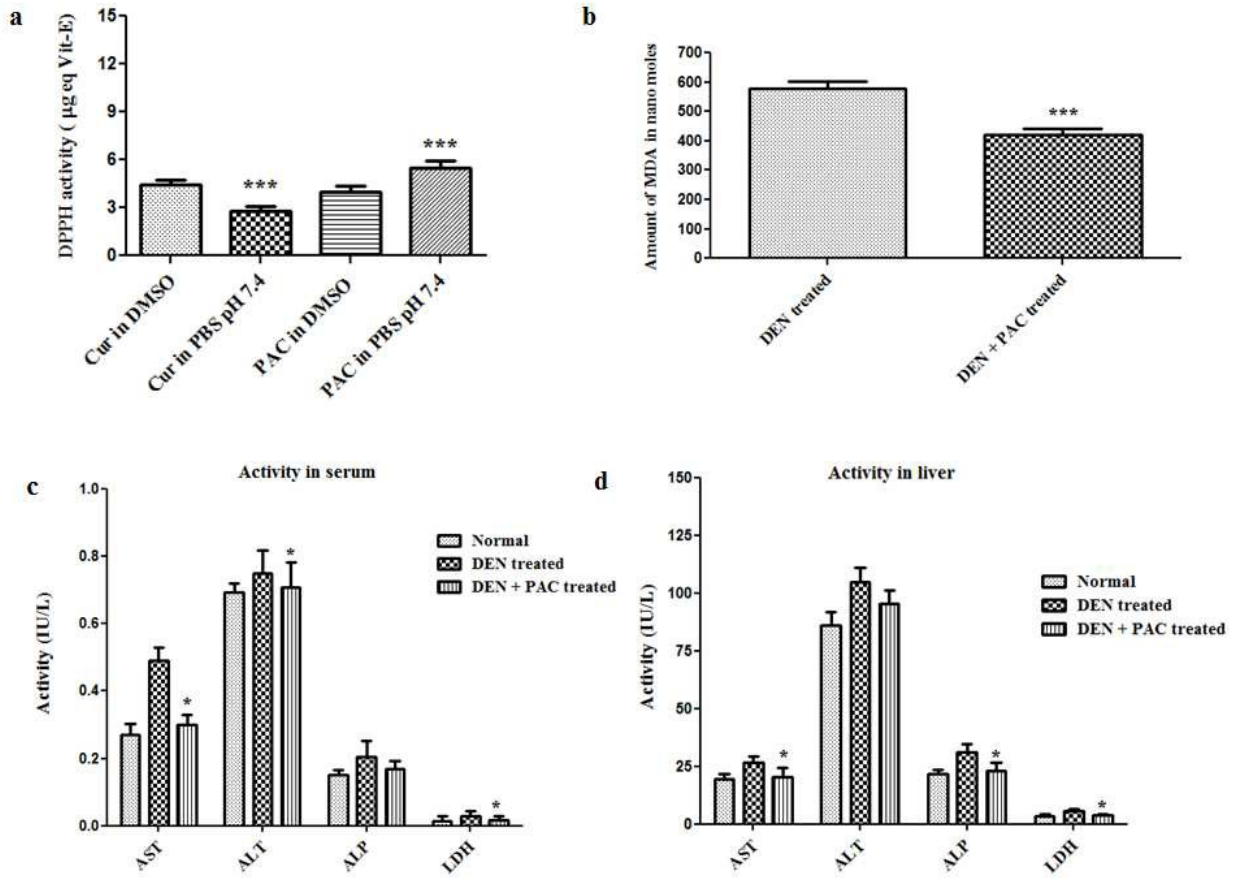

Figure 8

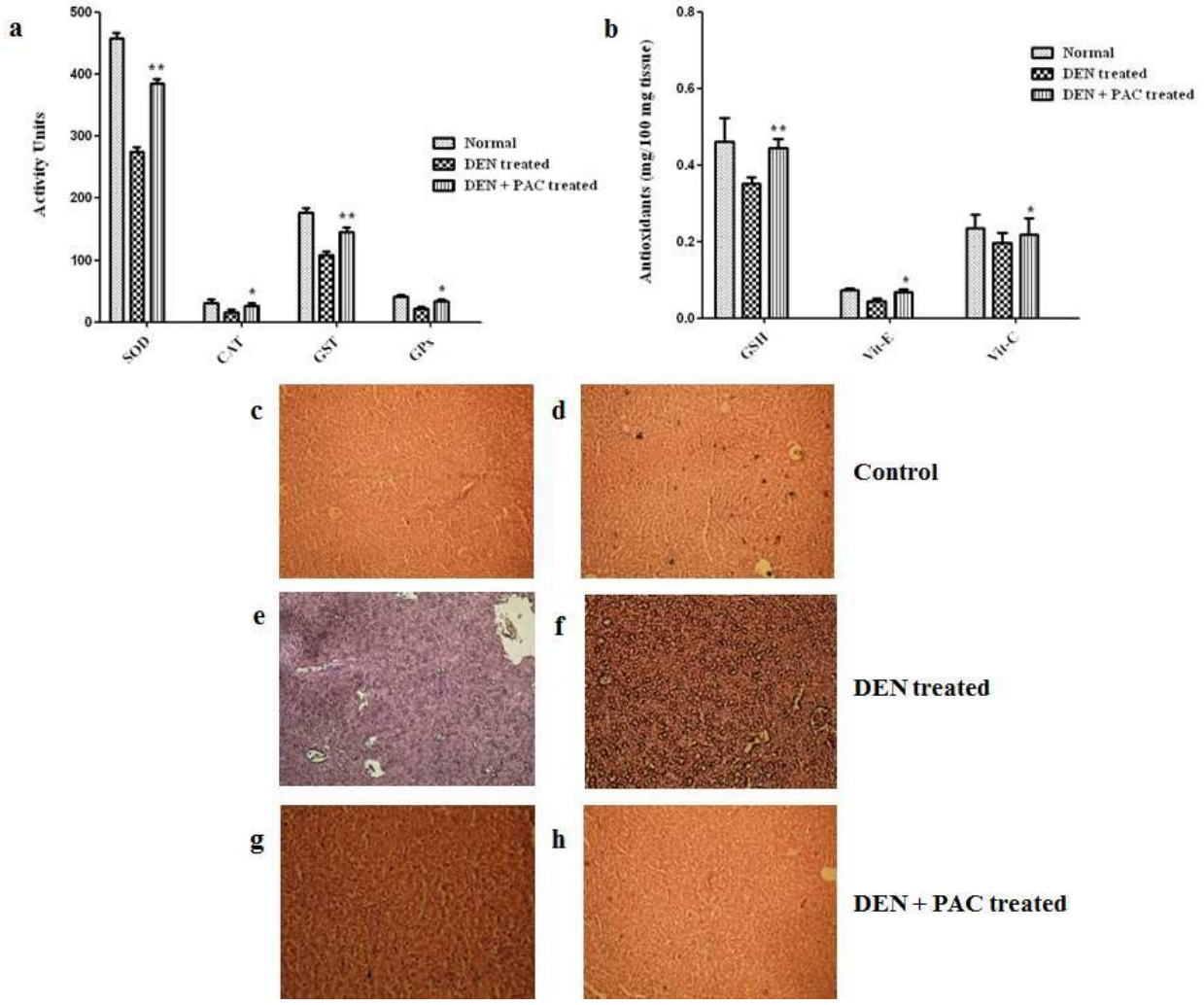

Graphical Abstract